Sādhanā Vol. 42, No. 4, April 2017, pp. 543–555
DOI 10.1007/s12046-017-0624-x

Experimental investigation of spray characteristics of kerosene and ethanol-blended kerosene using a gas turbine hybrid atomizer

AMLAN GARAI[1,*], SUBHADIP PAL[1,2], SUDEEPTA MONDAL[1,3], SHINJAN GHOSH[1,4], SWARNENDU SEN[1] and ACHINTYA MUKHOPADHYAY[1]

[1]Department of Mechanical Engineering, Jadavpur University, Kolkata 700032, India
[2]Department of Aerospace Engineering, Indian Institute of Technology Madras, Chennai 600036, India
[3]Department of Mechanical and Nuclear Engineering, Pennsylvania State University, State College, PA 16802, USA
[4]Department of Aerospace Engineering, University of Central Florida, Orlando, FL 32826, USA
e-mail: amlangarai@gmail.com

MS received 4 May 2016; revised 5 September 2016; accepted 7 November 2016

Abstract. Gas turbines have wide application as prime movers in transportation and power generating sectors, most of which are driven by fossil fuels like kerosene. The conventional fuels are associated with problems of air pollution, and the fuel reserves are getting depleted gradually. Addition of ethanol in kerosene leads to better spraying characteristics. The present work deals with the spray characteristics of pure kerosene and 10%-ethanol-blended (by volume) kerosene using a novel gas-turbine hybrid atomizer. Here the inner air and outer air enter in the same and opposite directions, respectively, with respect to the fuel flow direction into the atomizer and a high swirling effect occurs outside the nozzle. The fuel stream is sandwiched between two annular air streams and the flow rate of inner and outer air is varied continuously. Various spray stages like distorted pencil, onion, tulip and fully developed spray regimes have been observed. The breakup length, cone angle and sheet width of the fuel stream are analysed directly from backlit imaging for different fuel and air flow rates. From the image processing, it is observed that breakup occurs at an early stage for 10%-ethanol-blended kerosene due to low viscosity of ethanol. It is also observed that at higher air flow rate, breakup occurs at an early stage due to turbulent nature of the fuel stream.

Keywords. Atomization; breakup length (L_b); sheet width (SW); cone angle; kerosene blend; liquid sheet.

1. Introduction

Now-a-days, due to increasing demand of energy, the demand of fuel is also increasing rapidly. Most of the gas-turbine engines, heavy duty engines and earth movers are driven by petroleum-based fuel. But the declining resource of the fossil fuel and massive air pollution have led the researchers to find alternative fuels. Anthony *et al* [1] have stated that the alternative fuel should be profitable and its use should not adversely affect the power output and emission characteristics of the systems. Among different alternate sources of fuels, bioethanol appears to be a very promising choice for gas turbine combustors due to its ease of transportation and storage [2]. Bioethanol is, at present, the most widely used biofuel as it has been used in the transportation sector for a long time both in pure and in blended form [3]. Although alcohol has been widely investigated as an automotive fuel, there has been only limited number of studies on use of ethanol in gas turbine combustors. However, those studies have established the viability of ethanol as a gas turbine fuel. Moliere *et al* [4, 5] used bioethanol in heavy duty gas turbines and found superior emission characteristics compared with conventional fuels without any adverse effect on human safety and structural integrity. Alfaro-Ayala *et al* [6] showed that use of bioethanol as a gas turbine fuel produces lesser NO_x compared with conventional fuels like diesel and natural gas. However, fuel flow rate had to be increased to maintain the power output due to significant decrease in turbine inlet temperature. Sallevelt *et al* [7] compared the performance of bioethanol and diesel as gas turbine fuels. Bioethanol is chemically identical to ethanol; the difference lies only in the source of fuel. Thus ethanol can be a convenient surrogate for bioethanol in laboratory-scale studies. Alcohol, a low-viscosity fuel, which can be easily produced from crops, is proposed to maintain a balance between the demand and supply chain of fuel. Sayin [8] found that alcohol produces less emission due to its high

*For correspondence

stoichiometric air–fuel ratio, high oxygen content and low sulphur content. Khan *et al* [9] performed experiments for finding the thermal efficiency and fuel consumption rates of cooking stove using 5, 10, 15 and 20% ethanol in kerosene. Dioha *et al* [10] have also analysed the cooking stove performance by calculating the boiling time of specified volume of water using different ethanol–kerosene blends. Patra *et al* [11] studied the flame characteristics and combustor performance in a cylindrical spray combustor driven by kerosene and kerosene–ethanol blends. It is observed here that flame luminosity and brightness reduce considerably with increasing blend percentage of ethanol due to reduction of soot formation in flame.

Asfar and Hamed [12] found that blending ethanol reduces soot formation in the flame and emission of pollutants like CO, CO_2, NO_x and HC also reduces from the combustor. Khalil and Gupta [13] examined the distributed combustion characteristics using gaseous and liquid fuels. The gaseous fuels were methane, diluted methane, hydrogen-enriched methane and propane. The liquid fuels consisted of kerosene and ethanol. Lower NO and CO emissions were detected for the alternative fuels. Hence improved performance of the combustor can be achieved with the benefit of fuel flexibility, without any modifications to the injectors. CO emission was found to be lesser in blended fuel flames like biodiesel, diesel–biodiesel blends and emulsified bio-oils compared with diesel flames by Sequera *et al* [14]. Pure jet A fuel was blended with ethanol in varying volume fractions and performance characteristics along with emission characteristics were studied by Mendez *et al* [15, 16]. The same experiment was repeated by blending butanol with jet A fuel. Both the studies revealed lower emissions for CO and NO_x. Lower emissions were also detected in case of fossil fuel blends with four pure vegetable oils in an experiment performed on a 30 kWe commercial micro-gas turbine by Chiariello *et al* [17].

Ibrahim and Jog [18] revealed that counter-inner-co-outer swirling airstream has greater instability compared with Co-Inner–Counter-Outer configuration. By varying the flow condition, the aerodynamic breakup process of the liquid sheet can be analysed using an annular nozzle [19]. Chatterjee *et al* [20] investigated the breakup length, sheet expansion parameter and fractal dimension for kerosene using a hybrid atomizer with prefilming.

Finer droplets increase the rate of evaporation of fuel due to increase in the surface area. Hence combustor efficiency is improved due to finer droplet formation [21]. But larger droplets were found to have better penetration characteristics and hence better mixing was observed [22]. An optimum size for spray droplets for best combustor performance was found from a numerical study by Datta and Som [23].

Negeed *et al* [24] validated the breakup length, sheet velocity and droplet size of the liquid for a pressure swirl flat fan jet nozzle using a high-speed camera. Characteristics like input mean droplet diameters and spray cone angles are essential parameters to determine the performance of gas turbine combustors that use liquid fuels [25–29].

Many methods have been used in earlier works to capture the spray images before further image processing. Wahono *et al* [30] used a charged coupled device camera with a frame rate of 2000–3000 frames per second for their study on breakup of annular sheets. Duke *et al* [19] used a high-speed photography technique for measurements. The liquid phase had different characteristics of scattering as compared with the gaseous state. Hence proper contrast was obtained.

Pressure swirl and air-blast atomizers are the two types of atomizers used in gas-turbine engines. The former has the geometry composed of high-pressure liquid discharged into a slow moving environment, causing lot of soot formation. But the latter is a type of atomizer in which fuel is sandwiched between two annular air streams. The hybrid atomizer is the combination of the mentioned two types of atomizers [31, 32]. Now, the air-blast atomizer is a field of immense interest due to its reduced emission characteristics and reduced injection pressure. The present experiment is related to the spray characteristics of pure kerosene (KE0) and 10% ethanol (KE10) (by volume)-blended kerosene using an advanced gas-turbine hybrid atomizer.

2. Experimental set-up

The basic atomizer design with the dimensions is shown in figure 1. In this hybrid nozzle set-up, fuel and air enter tangentially and a high swirling effect occurs in the direction of the flow. By changing the direction of inner air stream with respect to the outer air stream, co- and counter-swirl effects are produced outside the atomizer. Swirl intensity is the ratio of momentum injected by the tangential inlet to the total momentum. An expression for swirl intensity with tangential inlet was derived by Leboucher *et al* [33]. The present experimental set-up also has tangential inlets for inner air, outer air and liquid. Leboucher *et al* [33] calculated and described the process of calculating the swirl intensity of two tangential inlets:

$$\text{swirl intensity for inner air} = \frac{1}{2}\left(\frac{\rho_i}{\rho_{it}}\right)\left(\frac{D_i^2}{D_{it}^2}\right)\left(\frac{m_{it}}{m_i}\right)$$

$$\text{swirl intensity for outer air and liquid} = \frac{1}{2}\left(\frac{\rho_i}{\rho_{it}}\right)\left(\frac{D_o^2 - D_i^2}{D_{it}^2}\right)\left(\frac{m_{it}}{m_i}\right).$$

These equations are used for calculating the swirl intensity of the inner air, outer air and liquid; ρ_i is the density of the air and fuel; ρ_{it} is the density of tangential inlet. In the present experimental process $\rho_i = \rho_{it}$; m_{it} is the mass flow of the tangential inlet and m_i is the total mass flow. The entire fuel and air come in through the tangential

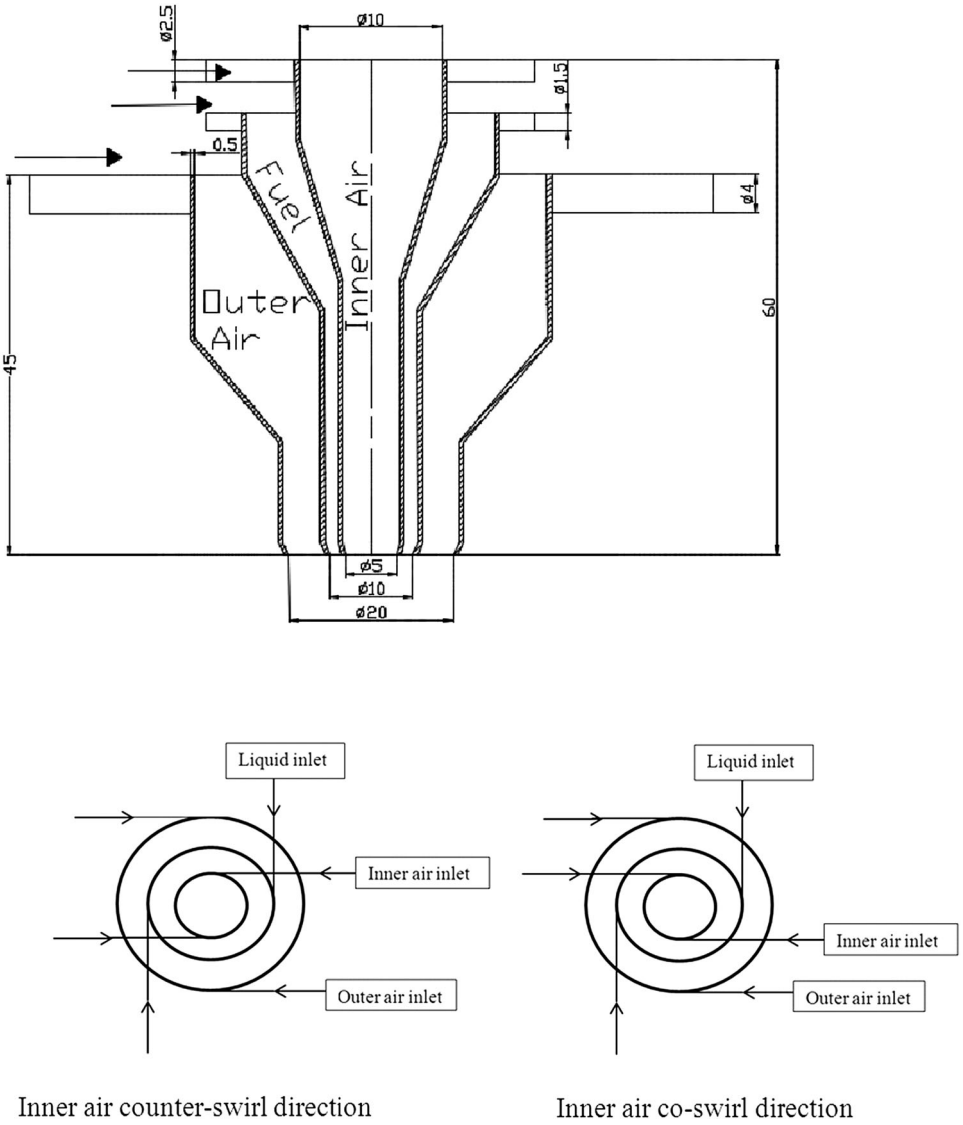

Figure 1. Atomizer schematic (dimensions in mm) (redrawn) [34].

inlet. Hence $m_i = m_{it}$. D_{it} is the diameter of the tangential inlet. In the present study D_{it} for inner air is 2.5 mm, outer air 4 mm and liquid 1.5 mm (given in figure 1). To calculate the inner air swirl intensity, D_i is taken as 5 mm. For calculating the outer air and liquid swirl intensity D_o is the outer diameter of the nozzle outlet and D_i is the inner diameter of the nozzle outlet. For the liquid swirl intensity, $D_o = 10$ mm and $D_i = 6$ mm are considered. For calculating the outer air swirl intensity, D_o is 20 mm and D_i is 11 mm. For the present experimental set-up, inner air and outer air swirl intensities are 2 and 8.7, respectively, and swirl intensity is 14.2 for liquid.

Air is fed to the atomizer by a compressor. A gear pump is used for the fuel flow through the set-up. The fuel and air flow rates are measured using rotameters (a 0–30 LPM kerosene rotameter was used for measuring the kerosene and 10%-ethanol-blended kerosene and a 0–50 LPM air rotameter was used for measuring the air flow rate). Figure 2 shows a schematic diagram of the experimental set-up. The compressor has been manufactured by ELGI Equipment LTD (Model SA OF 01 080 OF, displacement volume = 92 LPM), and this compressor is driven by a single-phase, 1 HP, 1450 rpm AC motor. The gear pump is driven by a single-phase 50 Hz 370 W 4.4 A ½ HP motor.

In the present work, a Prosilica high-speed (CV1280, Digital Machine Vision Camera, 1280 × 1024 monochrome, 1394 DCAM) camera is used to capture the spray images at 150 fps frame rate. Two 1000 W linear halogen lamps are used to create a diffuse backlighting system. A region of interest of 240 × 440 pixels was chosen to capture the required spray characteristics. A similar method of backlighting and high-speed imaging was used by Chatterjee *et al* [34].

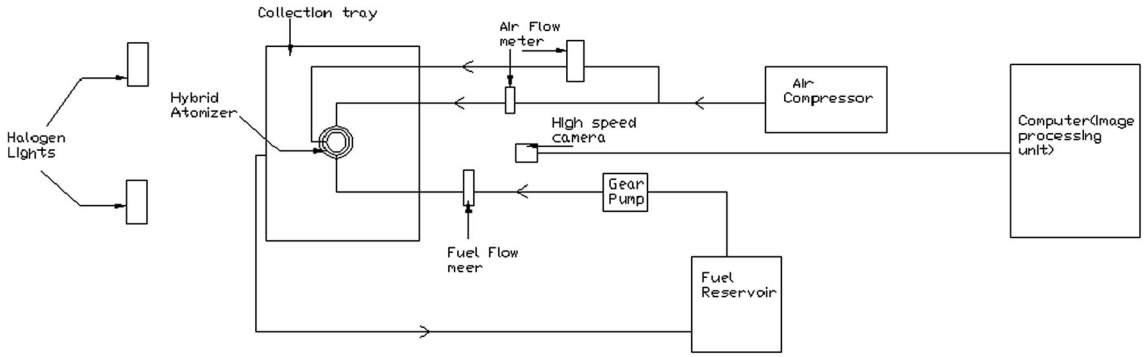

Figure 2. Schematic of experimental setup.

3. Blending

The blend is prepared at room temperature (30°C); 99.9% concentrated ethanol is used for the blending process. The non-polar hydrocarbons present in the kerosene oil have no affinity with the polar ethanol. The viscosity (kerosene 1.38 cSt and ethanol 1.14 cSt) and surface tension (kerosene 25.6 dyn/cm and ethanol 24.6 dyn/cm with a reference surface tension for water of 70 dyn/cm) of ethanol and kerosene are almost the same. Hence, following the work of Kim and Choi [35], 2% co-solvent tetrahydrofuran (C_4H_8O) is added into the kerosene-blended ethanol fuel to increase the stability of kerosene in ethanol. In this experimental work, 10% (by volume)-ethanol-blended kerosene (KE10) fuel is used.

4. Results and discussions

In this experiment, spray pattern, breakup length, sheet width and cone angle of 10%-ethanol-blended kerosene are studied and the results are compared with those for pure kerosene. Breakup length calculation is essential for the study of a gas turbine fuel injector, as breakup length determines the extent to which atomization occurs. Breakup is defined as the discontinuity in the sheet of liquid fuel, which produces ligaments and eventually droplets. Breakup is a complex, nonlinear, unsteady process. Early breakup is most desirable for combustion-related applications [36]. Breakup length is the axial distance from the outlet of the nozzle to the point where discontinuity in the sheet occurs. Sheet width is the maximum width of the liquid fuel sheet measured at an axial distance from the tip of the nozzle that is close to but lower than the breakup length. It gives us a measure of the amount of bulge in the fuel sheet. The sheet width can hence be related to the swirl of the three concentric streams of air and fuel, and how they interact to produce a final fuel spray due to hydrodynamics [34]. The cone angle is another important characteristic for an atomizer. It is defined as the angle between the two outer edges of the spray cone, as obtained in the snapshots. The greater the value of the spray cone, the more effective the spreading and dispersion of fuel droplets. Hence spray cone is a critical factor that determines the efficiency of the combustor [36]. The present study is done at inner air flow rates of 10, 20 and 30 LPM, both co-rotating and counter-rotating relative to the liquid stream, outer air flows of 0, 10, 20, 30, 40 and 50 LPM co-swirling relative to the fuel flow direction and fuel flow rate of 1 LPM.

Figure 3 shows the effect of outer air on the characteristics of spray with no inner air flow, so there is no effect of co- and counter-swirl on the fuel stream. At outer air flow rate of 0 LPM, the configuration is like that of a hollow jet. Consequently, the breakup morphology also resembles the classical instability mode of a liquid jet in air. As the inner air flow rate increases, the momentum transferred to the liquid sheet from the inner air jet increases the velocity of the former. This leads to ejection of droplets in the 'boundary layer stripping' mode before the disintegration of the sheet itself. At relatively high inner air flow rates of 40 and 50 LPM, the high momentum of the inner air jet destabilizes the liquid sheet very early and leads to disintegration of the sheet close to the nozzle itself. As the properties of the two fluids, kerosene and ethanol are very similar, the breakup characteristics of pure kerosene (KE0) and 10%-ethanol-blended fuel (KE10) are very similar. From the images, it is clear that at higher outer air flow rate, spray instability increases for both the fuels, but the ligament or droplet formation is higher in case of 10%-ethanol-blended fuel. We can come to this conclusion by studying the comparison of spray images, which have been obtained from high-speed imaging.

Figure 4 shows the effect of co- and counter-swirl of air on the fuel stream for increasing outer air flow rate at 1 LPM fuel flow rate. Different spray regimes have been observed from the snapshots. For both the fuels, at low outer air flow, onion and tulip shapes are produced. The onion regime is observed at low inner air flow rates and moderate outer air flow rates. The swirl in the inner air stream causes the liquid sheet to bulge outwards and delays

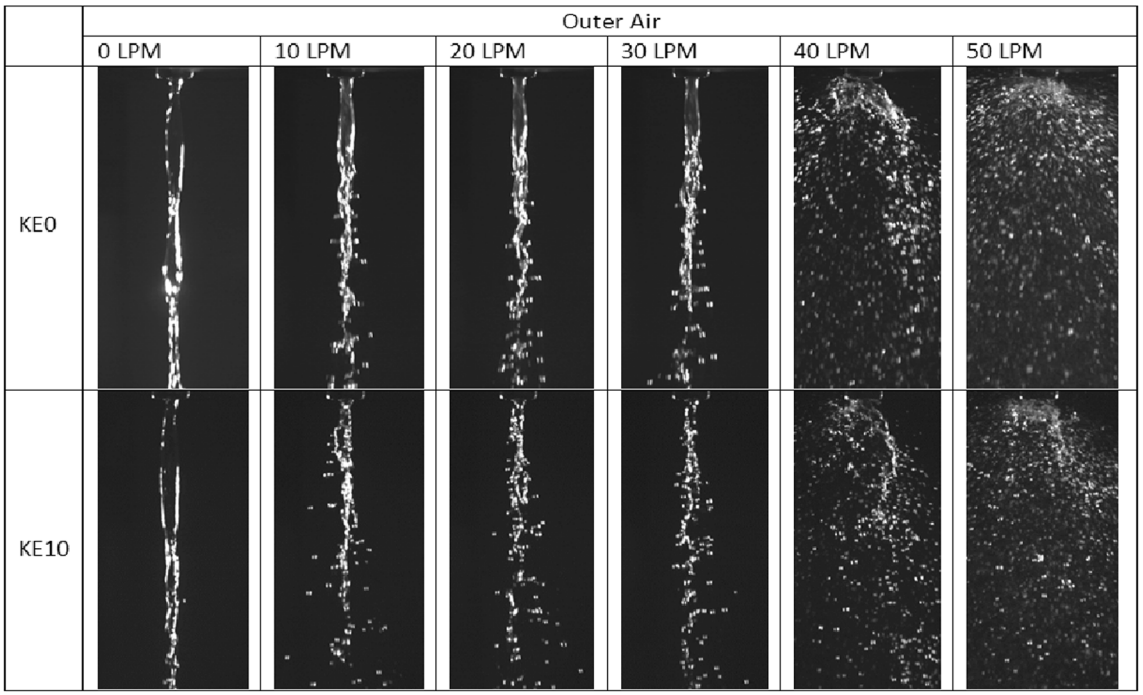

Figure 3. Spray image showing only outer air stream effect for kerosene and 10% ethanol blended fuel 1LPM liquid flow.

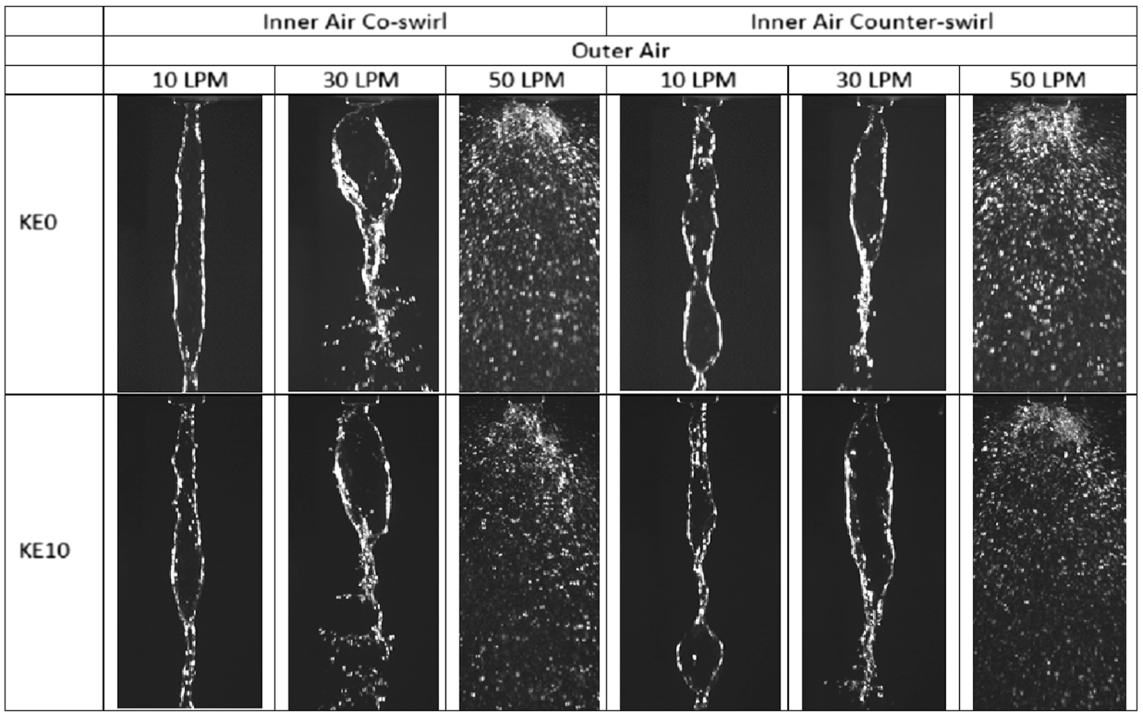

Figure 4. Spray image showing the 10 LPM inner air effect in co and counter swirl direction with increasing outer air flow in co swirl direction for kerosene and 10% ethanol blended fuel.

the breakup. At low inner and outer air flow rates (both 10 LPM and co-swirling with the liquid sheet), only a slight bulge of the jet is observed. As the outer flow rate increases, the higher strength of the outer swirling flow induces greater tangential momentum to the liquid sheet and causes a much greater bulge in the initial stages.

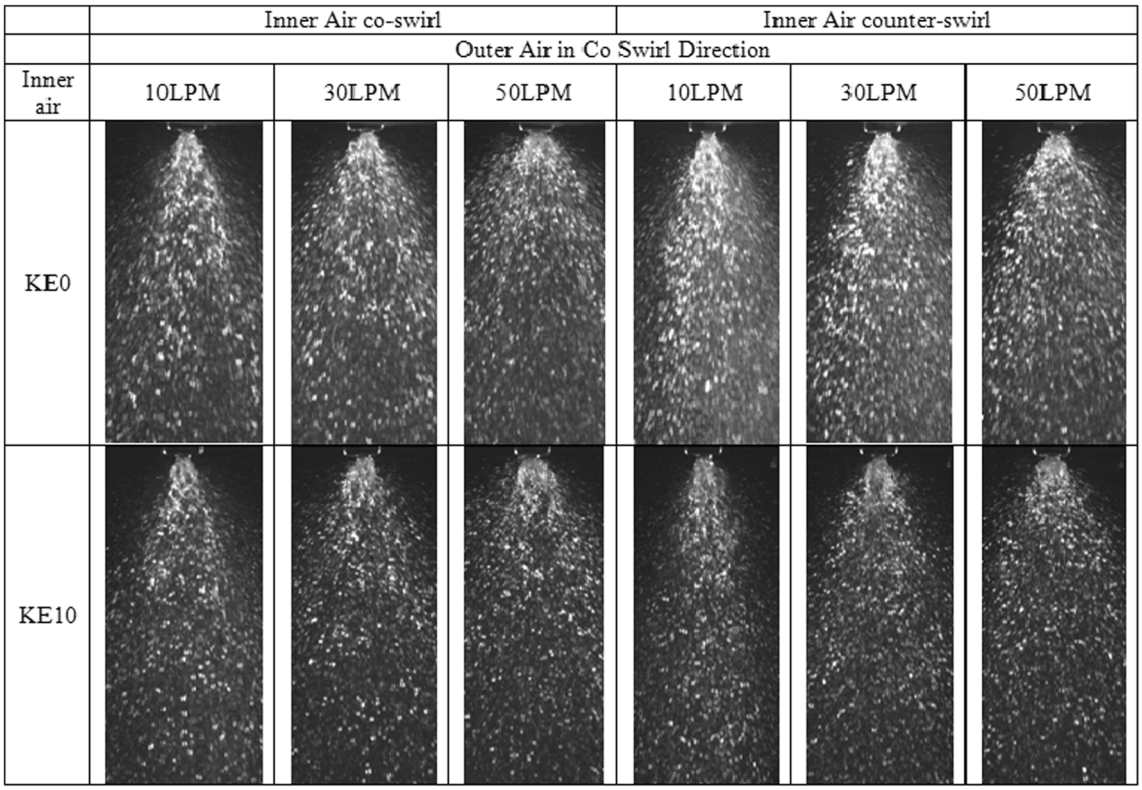

Figure 5. Spray image showing the 30 LPM inner air effect in co and counter swirl direction with increasing outer air flow in co swirl direction for kerosene and 10% ethanol blended fuel.

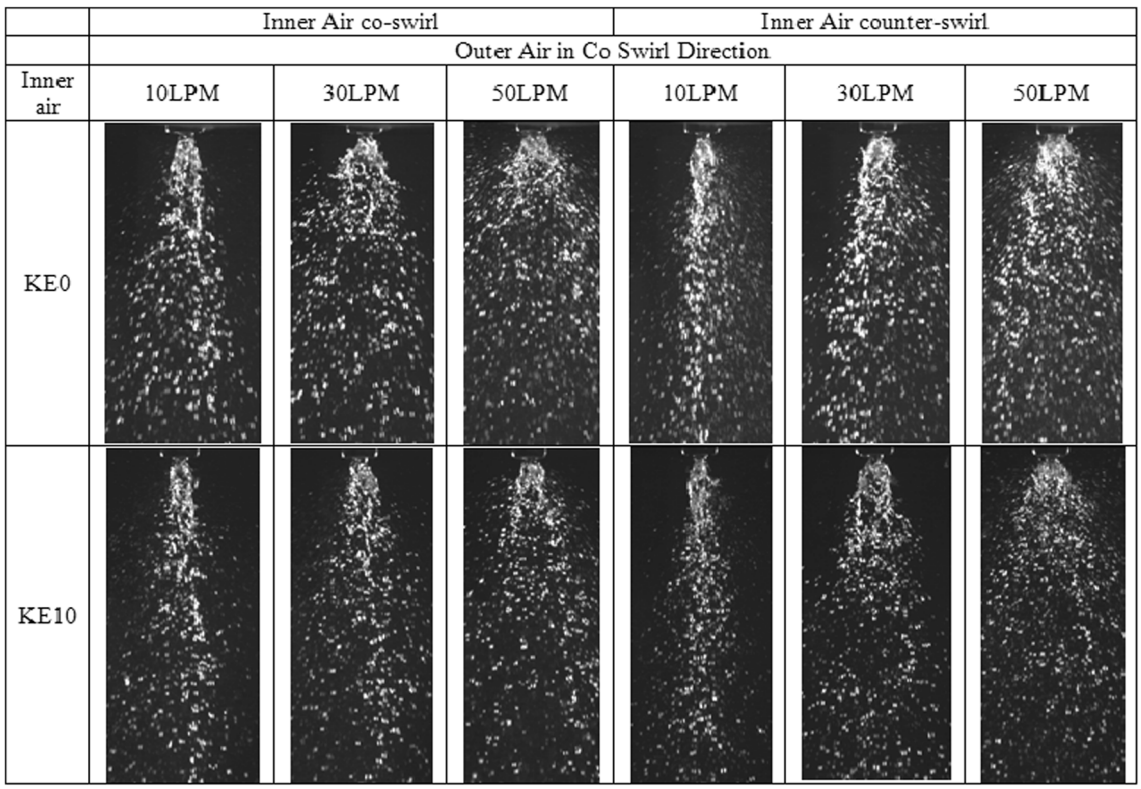

Figure 6. Spray image showing the 20 LPM inner air effect in co and counter swirl direction with increasing outer air flow in co swirl direction for kerosene and 10% ethanol blended fuel.

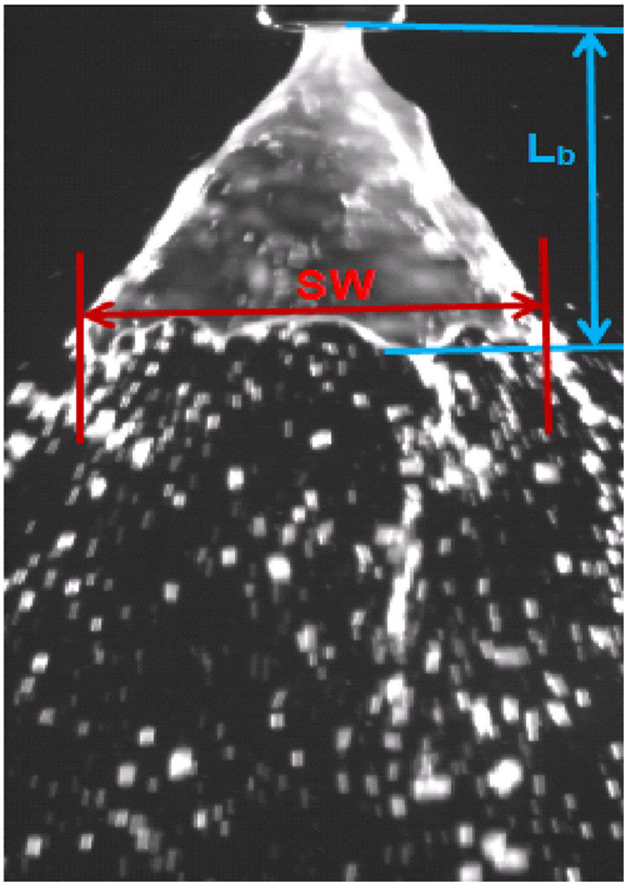

Figure 7. Typical spray image showing breakup length and sheet width.

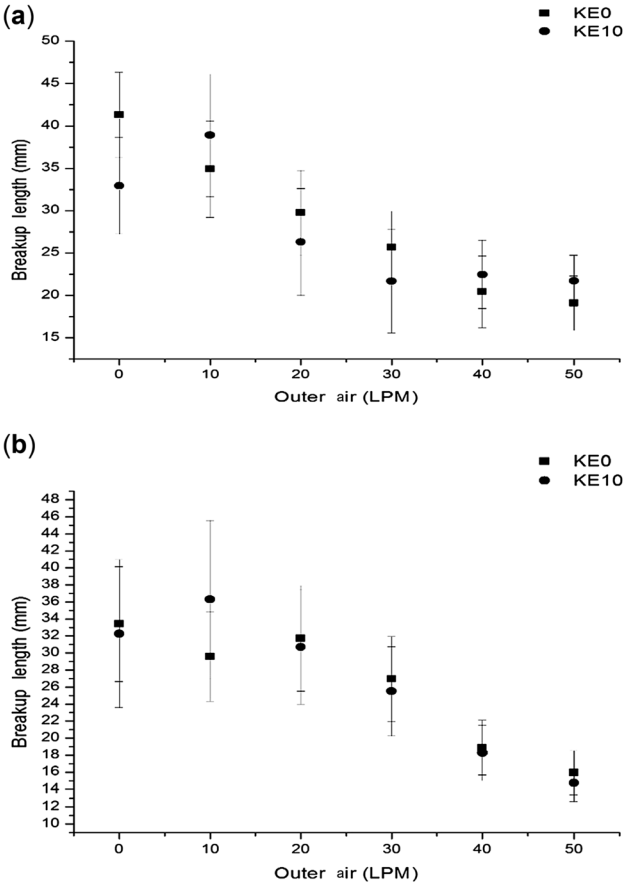

Figure 8. Variation of breakup length for Kerosene and 10% ethanol blended kerosene with increasing outer air flow in co swirl direction for co (**a**) and counter swirling (**b**) effect for 20LPM inner air flow and 1LPM fuel flow rate.

However, some distance downstream of the injector, the outer flow itself prevents further expansion of the liquid sheet and causes the bulge to collapse, giving rise to an onion shape. Onion shape is commonly observed in pressure-swirl atomizers where the swirling liquid sheet surrounds an air core whose velocity is not high. This is consistent with the observation of the onion shape at a low inner air flow rate. As the outer air flow rate increases, early breakup occurs very close to the nozzle exit. These regimes have been observed by Chatterjee *et al* [34] also. On the other hand, for the counter-swirling inner flow, the opposite directions of swirls on the two sides of the liquid sheet lead to modulation of the sheet along the axial direction. This gives rise to a necklace-like structure, particularly at low inner air flow rates and moderate outer air flow rates. A similar structure has been observed also by Zhao *et al* [37]. However in their configuration there was no outer air flow. Necklace formation is favourable for better spray characteristics. As the inner air flow rate increases to 20 and 30 LPM (figures 5 and 6), sufficient momentum is available from the inner stream itself to destabilize the liquid sheet and cause an early breakup at all outer air flow rates. From the spray images it is clear that both the outer and inner air play important roles in determining the spray characteristics of the hybrid atomizer. The differences in the geometric shapes formed in the spray images as well as the characteristics from the plot are visible for the two configurations.

The breakup length, the sheet width and the cone angle are calculated directly from the images obtained from the high-speed camera using Java-based image processing software ImageJ (developed by National Institutes of Health). Figure 7 shows the process for calculating the breakup length and sheet width from the spray image; 1000 frames were captured for each spray condition and ImageJ was used to calculate the spray characteristics for those frames. An average value was calculated for each condition using these values.

Figure 8 shows a comparison of breakup length for different outer air flow rates for kerosene and 10%-ethanol-blended kerosene. From the graph, it is clear that breakup length decreases with increasing outer air flow rate. For co-swirl configuration, breakup length is slightly lesser for pure kerosene, but for counter-swirl configuration, breakup length is almost similar for both the blends. However, at higher outer air flow rates, breakup length remains almost constant for co-swirl configuration and an increasing trend

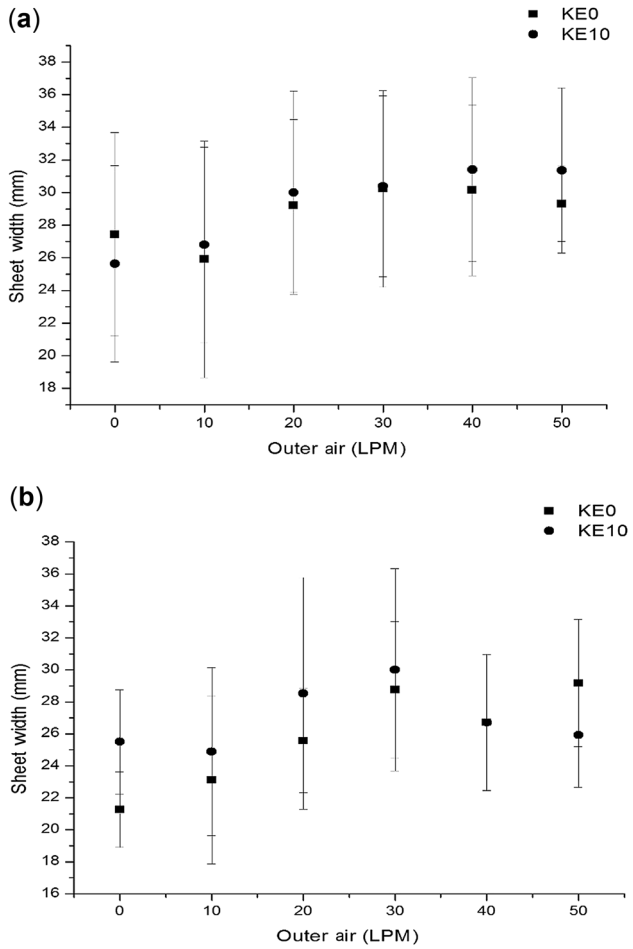

Figure 9. Variation of sheet width for Kerosene and 10% ethanol blended kerosene with increasing outer air flow in co swirl direction for co (**a**) and counter swirling (**b**) effect for 20LPM inner air flow and 1LPM fuel flow rate.

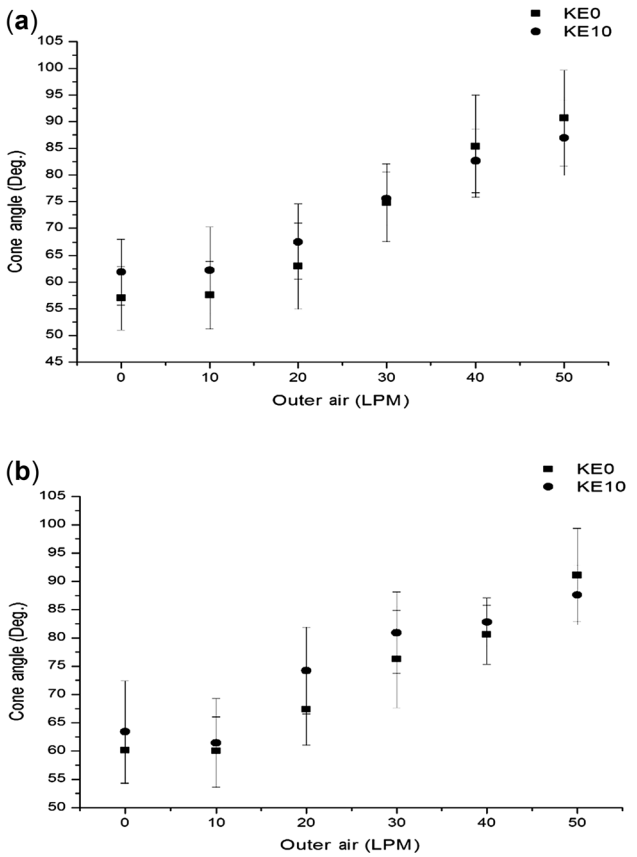

Figure 10. Variation of cone angle for Kerosene and 10% ethanol blended kerosene with increasing outer air flow in co swirl direction for co (**a**) and counter swirling (**b**) effect for 20 LPM inner air flow and 1LPM fuel flow rate.

is observed for counter-swirl configuration at low outer air flow rate.

Figure 9 shows the variation of sheet width for increasing outer air flow rate for kerosene and its 10% ethanol blend. With increasing outer air flow rate the sheet width increases, resulting in better spray characteristics. It is noted that sheet width is slightly higher for blended fuel and this comparison is more prominent in case of counter-swirl than the co-swirl configuration. At higher outer air flow rate, sheet width remains almost constant for co-swirl case, but a slight decreasing trend is noticed for counter-swirl case.

Figure 10 shows us the cone angle comparison between pure kerosene and alcohol–kerosene blend for the co-swirl and counter-swirl configurations for 20 LPM inner air flow. In figure 10a we find that for the co-swirl configuration, the cone angle value for KE10 blend is more than that of pure kerosene for 0–30 LPM outer air flow rate. However, at higher flow rates (40 and 50 LPM), we find that the value of cone angle for pure kerosene spray is slightly higher. In figure 10b, for the counter-swirl configuration, the cone angle for the blended fuel spray is found to be slightly higher than that of pure kerosene spray for all outer air flow rates except at the highest outer air flow rate of 50 LPM. Since cone angle gives us a fair idea about the extent of spreading of the spray cone, we can say that the KE10 fuel blend has marginally better droplet dispersion characteristics for most of the flow rates, except at the higher flow rates, where the pure kerosene spray is found to have a slightly higher cone angle.

4.1 *Effect of change in inner air flow rate*

Figure 11 shows a comparison of breakup length between the blended fuel and pure kerosene at 10 LPM inner air. For inner co-flow configuration, KE10 has lower breakup lengths for almost all the configurations. But in case of inner counter-flow, KE10 has better breakup characteristics at lower outer air flow rates, and at high flow rates (50–50 LPM), the breakup lengths of KE0 are found to be shorter. Sheet width plots (figure 12) reveal a lower value of sheet width for the KE10 fuel at almost all the outer air flow

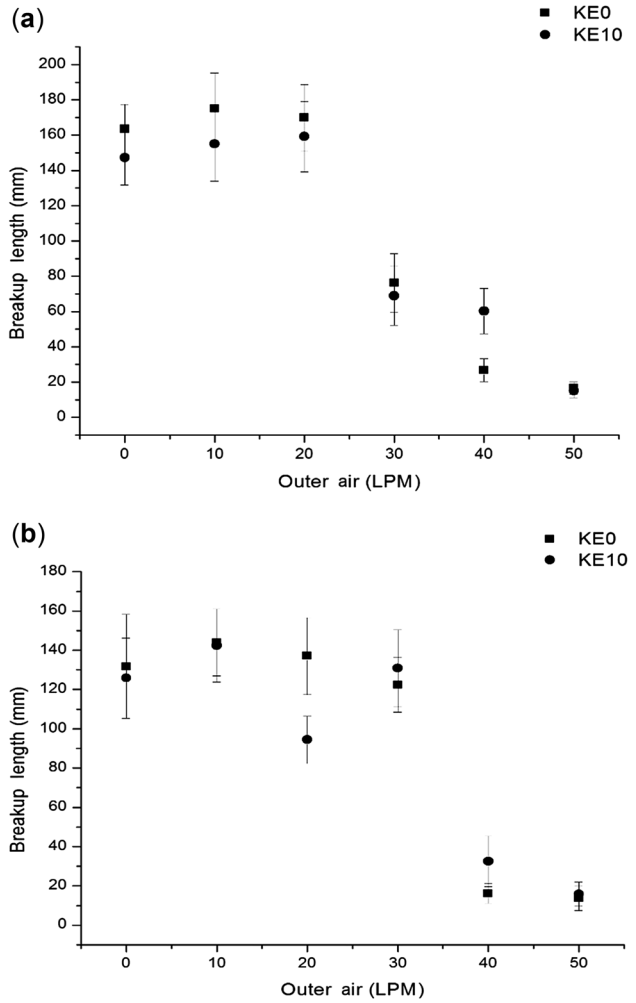

Figure 11. Variation of breakup length for Kerosene and 10% ethanol blended kerosene with increasing outer air in co swirl direction flow for co (**a**) and counter swirling (**b**) effect for 10LPM inner air flow and 1LPM fuel flow rate.

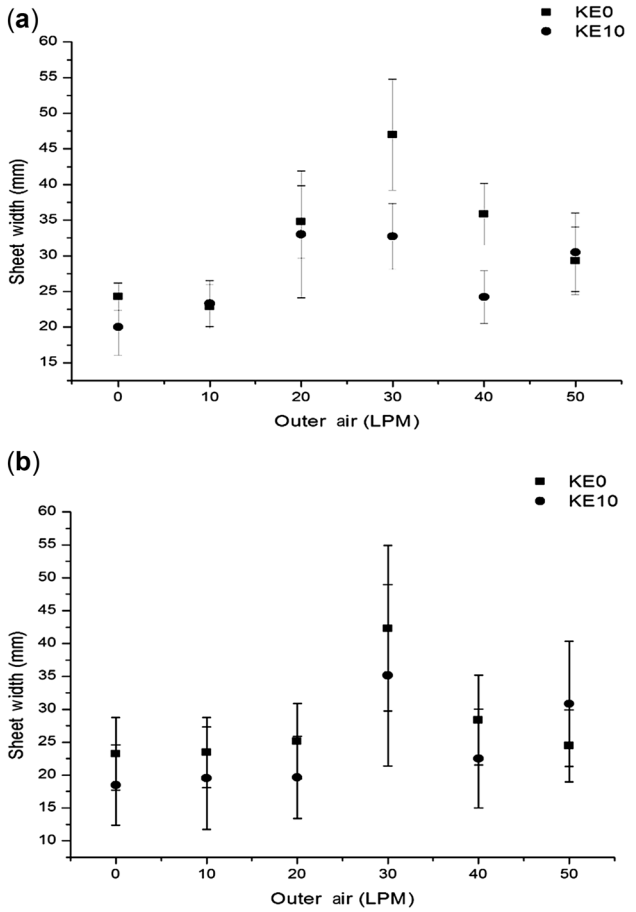

Figure 12. Variation of sheet width for Kerosene and 10% ethanol blended kerosene with increasing outer air flow in co swirl direction for co (**a**) and counter swirling (**b**) effect for 10LPM inner air flow and 1LPM fuel flow rate.

rates, for both co-flowing and counter-flowing (relative to the liquid) configurations. Cone angle measurements (figure 13) reveal that cone angle values are almost identical at lower flow rates (0–20 LPM) (figure 10a) for co-flowing inner air configuration and KE10 has higher cone angles at higher flow rates (30–50 LPM). On the other hand, counter-flowing inner air configuration has higher cone angles for all the flow rates of outer air. Hence from the combined effect of lower sheet width, lower breakup length and higher cone angles for most of the studied outer air flow rates, we can conclude that the KE10 fuel has better spraying characteristics.

With respect to the last case (20 LPM inner air flow), we have had a drop in the value of inner air flow rate. Hence by comparing the macroscopic spray characteristics, we can detect the changes due to variation of inner air flow rate. The range of variation of all the parameters is higher in the case of 10 LPM inner air flow rate. The gradient of cone angle and breakup lengths in the respective plots (figures 11 and 13) are steeper in case of inner 10 LPM air than those recorded for higher inner air flow rates. The sheet width plots in inner 20 LPM air (figure 9) showed almost constant curves. However, in the present case, the sheet widths follow an increasing pattern from 0–30 LPM and then a decreasing pattern at higher flow rates from 30–50 LPM.

Inner air flow rate was further increased to 30 LPM for study of spray characteristics. Again breakup length values (figure 14) were found to be quite close for the two fuels. For inner co-flow configuration, at lower outer air flow rates, breakup lengths were slightly lower for E10 blend. But with increase in flow rates, the two differences become even lesser. For inner counter-flow configuration (figure 14b), pure kerosene has lower breakup length than KE10 at 0–30 LPM. Again, at higher flow rates, the two breakup length values become almost identical. Sheet width plots (figure 15) show lower sheet width for pure kerosene at all flow rates in the Outer-Co–Inner-Co configuration. At inner counter, sheet width of KE10 fuel is lower at low flow rates and higher at high flow rates (40–50 LPM). Cone angle values of Outer-Co–Inner-Co configuration are

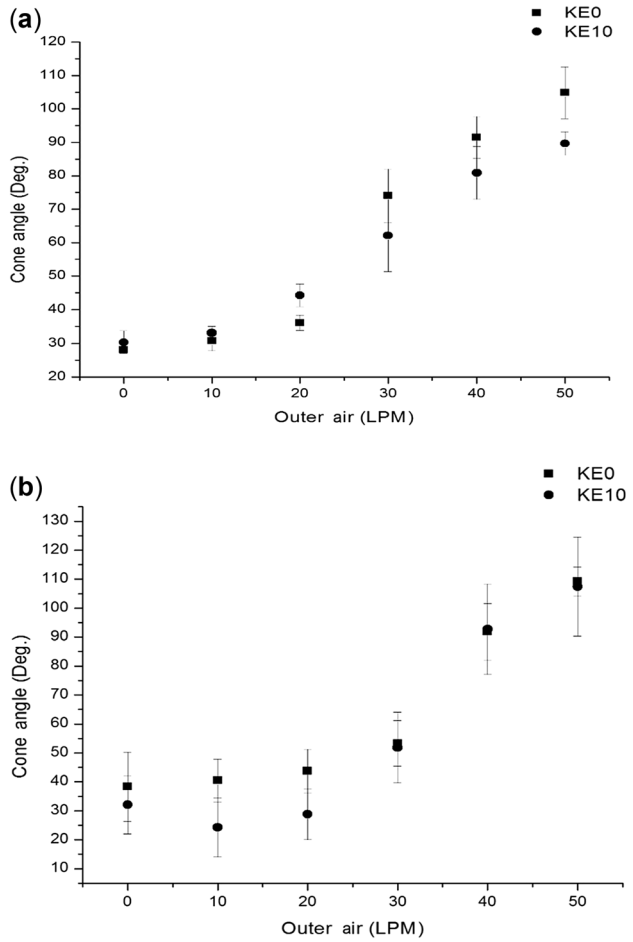

Figure 13. Variation of cone angle for Kerosene and 10% ethanol blended kerosene with increasing outer air flow in co swirl direction for co (**a**) and counter swirling (**b**) effect for 10 LPM inner air flow and 1LPM fuel flow rate.

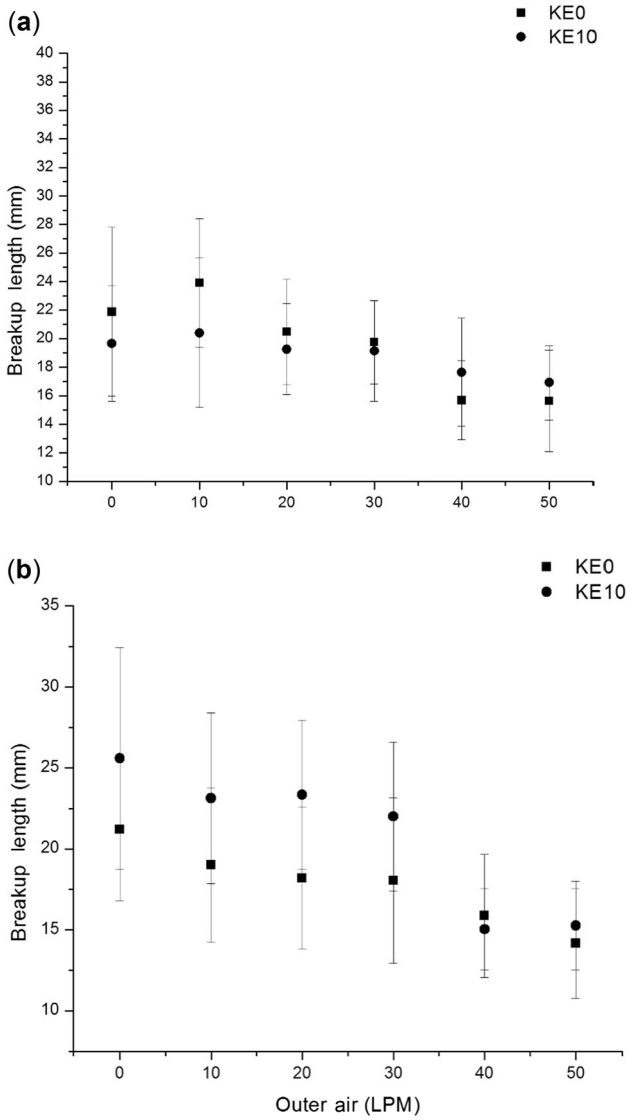

Figure 14. Variation of break-up length for Kerosene and 10% ethanol blended kerosene with increasing outer air flow in co swirl direction, for co (**a**) and counter swirling (**b**) effect for 30LPM inner air flow and 1LPM fuel flow rate.

higher for KE10 fuel blends compared with KE0 in figure 16. For Outer-Co–Inner-Counter configuration, KE0 cone angles are greater at low outer air flow rates and at high flow rates (30–50 LPM) the cone angles are almost identical in magnitude. Quality of atomization can be judged as slightly better for KE10 in case of inner-co configuration at low flow rates. However, at higher flow rates both the fuels show almost equivalent characteristics. Similarly in Inner-Counter–Outer-Co configuration, KE0 has better breakup characteristics at lower flow rates, but at higher flow rates (30–50 LPM), both the fuels show almost the same behaviour.

An increase in inner air flow rate to 30 LPM again reduces the range of values of the parameters measured. For example, in this case we observe a small change in values of breakup length with increase in flow rates of outer air stream. The 10 LPM case had the highest range in values of the spray characteristics as the flow regime changed from onion, tulip or jet to early breakup with increase in air flow rates (figures 3 and 4). Changes in flow regimes have a considerable effect upon spray characteristics, especially breakup length. While onions are stable swirling shapes with high breakup length, early breakup modes have low breakup lengths. However, in case of higher inner air flow rates we get a fully developed spray cone with early breakup even in cases of low outer air flow rates. Hence the changes observed are not very significant. Figures 5 and 6 show fully developed spray cones undergoing early breakup, for 20 and 30 LPM inner air flow.

5. Conclusions

An experimental investigation of spray formation has been performed for conventional kerosene fuel, and a kerosene–ethanol blend. The breakup length, sheet width and cone

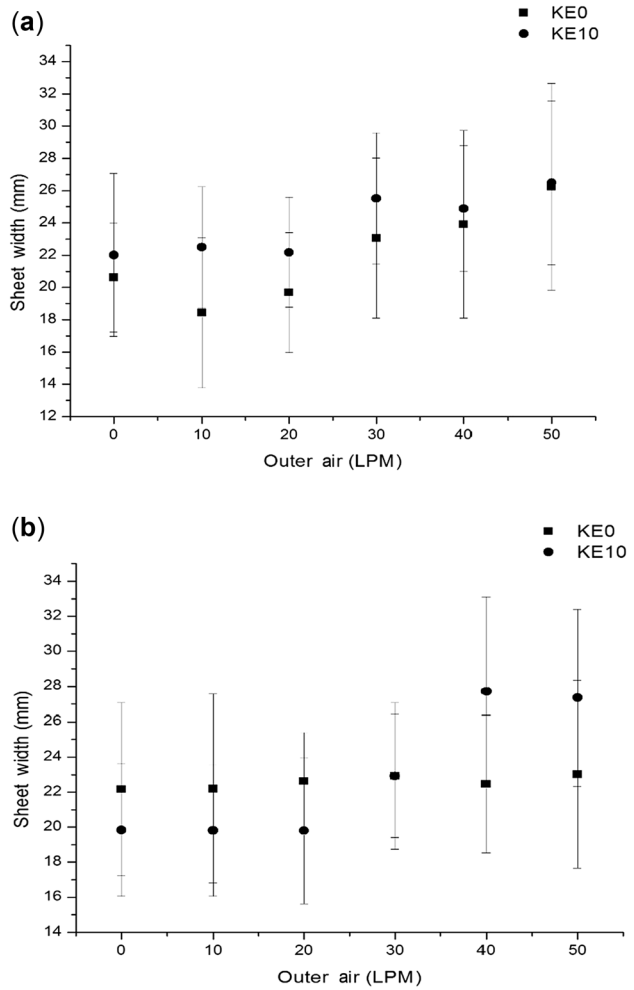

Figure 15. Variation of sheet width for Kerosene and 10% ethanol blended kerosene with increasing outer air flow in co swirl direction for co (**a**) and counter swirling (**b**) effect for 30LPM inner air flow and 1LPM fuel flow rate.

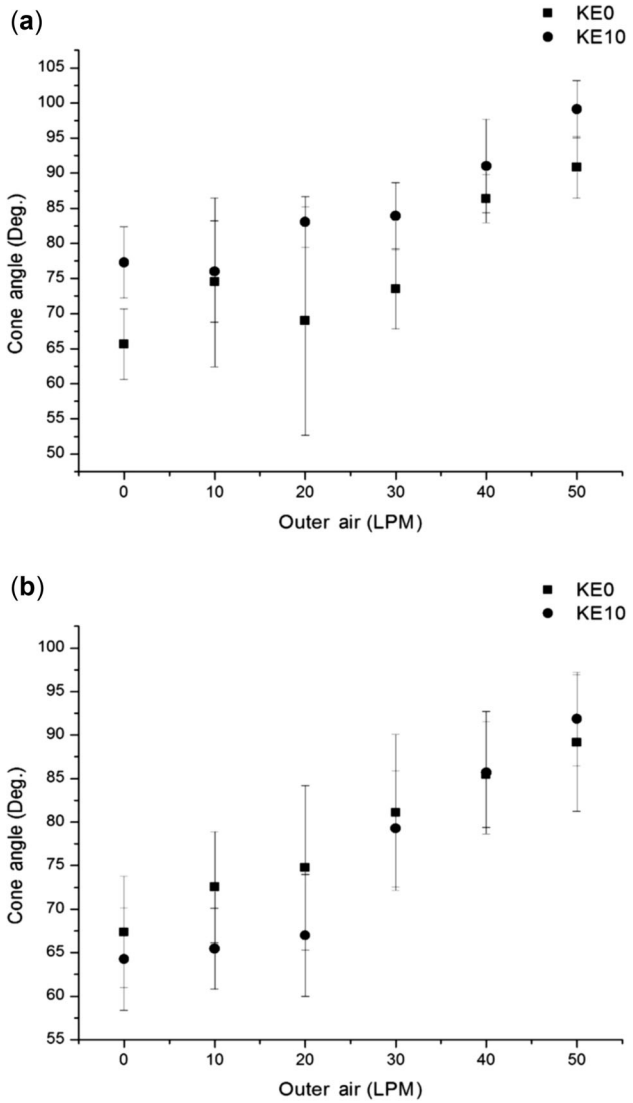

Figure 16. Variation of cone angle for Kerosene and 10% ethanol blended kerosene with increasing outer air flow in co swirl direction for co (**a**) and counter swirling (**b**) effect for 30 LPM inner air flow and 1LPM fuel flow rate.

angle have been measured for different flow configurations, which provide an idea of the macroscopic spray characteristics. It has been found that addition of ethanol has an overall effect of reducing the breakup length and increasing the sheet width of the spray regime, thereby indicating better spraying characteristics of the blended fuel. The effect of breakup length has been found to be more prominent in the co-swirling configuration while the effect of sheet width is more clear in case of counter-swirling configuration, indicating its higher effectiveness for low air-flow atomization. Cone angle measurements show that the kerosene–ethanol blend has higher cone angles compared with pure kerosene for most of the flow conditions. The variation of inner air flow rate shows that with higher flow rates, the changes in measured parameters with increase in outer air flow rates are lesser. Further, it can be concluded that detachment fuel droplet in fuel stream prior to breakup increases in case of ethanol-blended kerosene in some cases and the breakup characteristics are quite similar for both the fuels in the other instances. Hence quality of atomization, in general, is not adversely affected by adding ethanol to kerosene. Thus while blending with ethanol is beneficial from the viewpoint of sustainability, conserving fossil fuel reserve and reducing emissions, similar atomization characteristics imply good fuel flexibility for the injectors. Hence injectors designed for kerosene can be conveniently used for kerosene–ethanol blends also.

Acknowledgement

The financial supports of Gas Turbine Research Establishment (GTRE) under the GATET scheme and Defence Research and Development Organization (DRDO),

Government of India, are gratefully acknowledged. Help from Mr. Souvick Chatterjee in developing the image processing techniques is gratefully acknowledged. One author (AG) gratefully acknowledges fellowship from Technical Education Quality Improvement Programme (TEQIP-II) of Government of India.

References

[1] Anthony C, Jeffrey G, Tim H, Roy W, Michel M and Joseph C 2008 New York: American Society of Mechanical Engineers

[2] Goodger E M 2000 *Transport fuel technology*. Norwich, UK: Landfall Press

[3] Balat M and Balat H 2009 Recent trends in global production and utilization of bio-ethanol fuel. *Appl. Energy* 86: 2273–2282

[4] Moliere M, Vierling M, Aboujaib M, Patil P, Eranki A, Campbell A, Trivedi R, Nainani A, Roy S and Pandey N 2009 Gas turbine in alternative fuel application: bioethanol field test. In: *Proceedings of ASME Turbo Expo*, Orlando, Florida

[5] Moliere M, Panarotto E, Aboujaib M, Bisseaud J M, Campbell A, Citeno J, Maire P A and Ducrest L 2007 Gas turbine in alternative fuel application: bio-diesel field test. In: *Proceedings of ASME Turbo Expo*, Montreal, Canada

[6] Alfaro-Ayala J A, Gallegos-Muñoz A, Uribe-Ramirez A R and Belman J M 2013 Use of bioethanol in a gas turbine combustor. *Appl. Therm. Eng.* 61: 481–490

[7] Sallevelt J L H P, Pozarlik A K, Beran M, Axelsson L U and Brem G 2014 Bioethanol combustion in an industrial gas turbine combustor: simulations and experiments. *ASME J. Eng. Gas Turbines Power* 136: 071501-1–071501-8

[8] Sayin C 2010 Engine performance and exhaust gas emissions of methanol and ethanol-diesel blends. *Fuel* 89: 3410–3415

[9] Khan M Y, Khan F A and Beg M S 2013 Ethanol–kerosene blends: Fuel option for kerosene wick stove. *Int. J. Eng. Res. Appl.* 3: 464–466

[10] Dioha I J, Ikeme C H, Tijjani N and Dioha E C 2012 Comparative studies of ethanol and kerosene fuels and cook stoves performance. *J. Nat. Sci. Res.* 2: 34–39

[11] Patra J, Ghose P, Datta A, Das M, Ganguly R, Sen S and Chatterjee S 2015 Studies of combustion characteristics of kerosene ethanol blends in an axi-symmetric combustor. *Fuel* 144: 205–213

[12] Asfar K R and Hamed H 1998 Combustion of fuel blends. *Energy Convers. Manage.* 39: 1081–1093

[13] Khalil A E E and Gupta A K 2013 Fuel flexible distributed combustion for efficient and clean gas turbine engines. *Appl. Energy* 109: 267–274

[14] Sequera D, Agrawal A K, Spear S K and Daly D T 2008 Combustion performance of liquid biofuels in a swirl-stabilized burner. *J. Eng. Gas Turb. Power—Trans. ASME* 130: 032810–032818

[15] Mendez C J, Parthasarathy R N and Gollahalli S R 2012 Performance and emission characteristics of a small scale gas turbine engine fueled with ethanol/Jet A blends. In: *Proceedings of the 50th Aerospace Sciences Meeting*, AIAA, Nashville, Tennessee, AIAA 2012–0522

[16] Mendez C J, Parthasarathy R N and Gollahalli S R 2014 Performance and emission characteristics of butanol/Jet A blends in a gas turbine engine. *Appl. Energy* 118: 135–140

[17] Chiariello F, Allouis C, Reale F and Massolia P 2014 Gaseous and particulate emissions of a micro gas turbine fueled by straight vegetable oil–kerosene blends. *Exp. Therm. Fluid Sci.* 56: 16–22

[18] Ibrahim A A and Jog M A 2006 Effect of liquid and air swirl strength and relative rotational direction on the instability of an annular liquid sheet. *Acta Mech*. 186: 113–133

[19] Duke D, Honnery D and Soria J 2010 A cross-correlation velocimetry technique for breakup of an annular liquid sheet. *Exp. Fluids* 49: 435–445

[20] Chatterjee S, Das M, Mukhopadhyay A and Sen S 2014 Effect of geometric variations on the spray dynamics of an annular fuel sheet in a hybrid atomizer. *Atomization Spray* 24: 673–694

[21] Lefebvre A H 1985 Fuel effects on gas turbine combustion—Ignition, stability and combustion efficiency. *J. Eng. Gas Turbines Power: Trans. ASME* 107: 24–37

[22] Odgers J, Kretschmer D and Pearce G F 1993 The combustion of droplets within gas turbine combustors: Some recent observations on combustion efficiency. *J. Eng. Gas Turbines Power: Trans. ASME* 115: 522–532

[23] Datta A and Som S K 1999 Combustion and emission characteristics in a gas turbine combustor at different pressure and swirl conditions. *Appl. Therm. Eng.* 19: 949–967

[24] Negeed E S R, Hidaka S, Kohno M and Takata Y 2011 Experimental and analytical investigation of liquid sheet breakup characteristics. *Int. J. Heat Fluid Flow* 32: 95–106

[25] Banhawy Y E and Whitelaw J H 1981 Experimental study of the interaction between a fuel spray and surrounding combustion air. *Combust. Flame* 42: 253–275

[26] Jones W P and Toral H 1983 Temperature and composition measurement in a research gas-turbine combustion chamber. *Combust. Sci. Technol.* 31: 249–275

[27] Heitor M V and Whitelaw J H 1986 Velocity, temperature and species characteristics of the flow in a gas turbine combustor. *Combust. Flame* 64: 1–32

[28] Bicen A F, Senda M and Whitelaw J H 1989 Scalar characteristics of combusting flow in a model annular combustor. *J. Eng. Gas Turbines Power: Trans. ASME* 111: 90–96

[29] Cameron C D, Brouwer J, Wood C P and Samuelsen G S 1989 A detailed characterization of the velocity and thermal fields in a model can combustor with wall jet injection. *J. Eng. Gas Turbines Power: Trans. ASME* 111: 31–35

[30] Wahono S, Honnery D, Soria J and Ghojel J 2008 High-speed visualisation of primary break-up of an annular liquid sheet. *Exp. Fluids* 44: 451–459

[31] Chin J S, Rizk N K and Razdan M K 1999 Study on hybrid air blast atomization. *J. Propul. Power* 15: 241–247

[32] Rizk N K, Chin J S and Razdan M K 1996 *Influence of design configuration on hybrid atomizer performance*. AIAA Paper 96-2628

[33] Leboucher N, Roger F and Carreau J L 2010 Disintegration process of an annular liquid sheet assisted by coaxial gaseous coflow(s). *Atomization Spray* 20: 847–862

[34] Chatterjee S, Das M, Mukhopadhyay A and Sen S 2015 Experimental investigation of breakup of annular liquid sheet in a hybrid atomizer. *J. Propul. Power* 31 1232–1241

[35] Kim H and Choi B 2008 Effect of ethanol–diesel blend fuels on emission and particle size distribution in a common-rail direct injection diesel engine with warm-up catalytic converter. *Renew. Energy* 33: 2222–2228

[36] Fu Q F, Yang L J, Qu Y Y and Gu B 2010 Linear stability analysis of a conical liquid sheet. *J. Propul. Power* 26: 955–967

[37] Zhao H, Xu J L, Wu J H, Li W F and Liu H F 2015 Breakup morphology of annular liquid sheet with an inner round air stream. *Chem. Eng. Sci.* 137: 412–422